Enzootic and epizootic dynamics of the chytrid fungal pathogen of amphibians

Cheryl J. Briggs[a,1], Roland A. Knapp[b], and Vance T. Vredenburg[c]

[a]Department of Ecology, Evolution and Marine Biology, University of California, Santa Barbara, CA 93106; [b]Sierra Nevada Aquatic Research Laboratory, University of California, Mammoth Lakes, CA 93546; and [c]Department of Biology, San Francisco State University, San Francisco, CA 94132

Edited* by David B. Wake, University of California, Berkeley, CA, and approved April 12, 2010 (received for review November 9, 2009)

Chytridiomycosis, the disease caused by the chytrid fungus, *Batrachochytrium dendrobatidis* (Bd), has contributed to amphibian population declines and extinctions worldwide. The impact of this pathogen, however, varies markedly among amphibian species and populations. Following invasion into some areas of California's Sierra Nevada, Bd leads to rapid declines and local extinctions of frog populations (*Rana muscosa*, *R. sierrae*). In other areas, infected populations of the same frog species have declined but persisted at low host densities for many years. We present results of a 5-year study showing that infected adult frogs in persistent populations have low fungal loads, are surviving between years, and frequently lose and regain the infection. Here we put forward the hypothesis that fungal load dynamics can explain the different population-level outcomes of Bd observed in different areas of the Sierra Nevada and possibly throughout the world. We develop a model that incorporates the biological details of the Bd-host interaction. Importantly, model results suggest that host persistence versus extinction does not require differences in host susceptibility, pathogen virulence, or environmental conditions, and may be just epidemic and endemic population dynamics of the same host–pathogen system. The different disease outcomes seen in natural populations may result solely from density-dependent host–pathogen dynamics. The model also shows that persistence of Bd is enhanced by the long-lived tadpole stage that characterize these two frog species, and by nonhost Bd reservoirs.

amphibian decline | *Batrachochytrium dendrobatidis* | chytridiomycosis | emerging infectious disease | host–pathogen dynamics

Chytridiomycosis, caused by the fungal pathogen *Batrachochytrium dendrobatidis* (Bd), has been called the "worst infectious disease ever recorded among vertebrates in terms of the number of species impacted, and its propensity to drive them to extinction" (1). Since it was first identified in the late 1990s (2, 3), Bd has been found in almost every region in which researchers have searched. It is now nearly global in its distribution, and it has been implicated in dramatic declines in amphibian populations worldwide (4, 5). One of the most striking features of this pathogen, however, is the variability in outcome of infection that has been observed among species, and among populations within a species. Chytridiomycosis leads to the rapid death of individuals of some species (2, 6, 7), whereas individuals of other species develop only minor infections and suffer little or no negative effects (8, 9). A number of factors, including temperature (10), innate defenses (11, 12), habitat (13, 14), and host life history traits (15), have been demonstrated to contribute to the variable outcomes of Bd infection.

Bd is currently having a devastating impact on populations of frogs in the mountain yellow-legged frog species complex (*Rana muscosa* and *R. sierrae*) in parts of the Sierra Nevada Mountains of California (6, 16). In Sequoia and Kings Canyon National Parks, we have documented the first appearance of Bd in many watersheds, resulting in the rapid decline of the frog populations (6, 16). The majority of these population crashes have caused the extirpation of all frog populations in the affected areas. However, a few populations, although reduced greatly in numbers after Bd arrival, were not extirpated (even those located adjacent to areas in which all frog populations have been extirpated). These mountain yellow-legged frog populations continue to be infected with Bd, but appear to be persisting with the fungus (17). In Yosemite National Park, the initial arrival of Bd was not observed; Bd has been present for at least a decade (18, 19). The remaining frog populations are all infected with Bd, but many appear to be persisting in the long term. Such vastly different dynamical outcomes of a pathogen (rapid extirpation vs. long-term persistence) suggest differences in the host–pathogen interaction at the different sites, for example, differences in frog susceptibility or fungal virulence. Here we propose that these types of differences might not be necessary to explain the observed varying outcomes of infection.

Mountain yellow-legged frogs occur only in high-elevation lakes and streams (above 1,500 m) in California. All stages of the frogs are aquatic, and in the Sierra Nevada, frogs spend 8–9 months of the year overwintering under ice. The tadpole stage is unusually long-lived, lasting 1–4 years. Although once abundant, these frogs have disappeared from most of their historic range during the past several decades (20). The spread of Bd is a major factor driving this decline (6, 16), with *R. muscosa* known to be infected with Bd since at least the 1970s (19).

Bd infects keratinized tissues of amphibians, specifically the skin of postmetamorphic stages and mouth parts of larval stages (3, 21). Bd is transmitted via an aquatic flagellated zoospore (21, 22). Zoospores are thought to infect cells within the stratum granulosum either directly or via a germ tube and then develop into sporangia (3, 21). After a temperature-dependent number of days, the sporangium releases zoospores through a discharge papilla (21, 23). Berger (21) showed through electron microscopy that discharge papillae usually point to the skin surface, suggesting that most zoospores are released to the outer surface of the skin, although some zoospores might stay within skin layers and potentially cause self-reinfection. Whereas other chytrid fungi have a sexual stage resulting in a thick-walled resistant sporangium, such a stage has not yet been identified in Bd (but see ref. 24). Bd usually has little detectable negative effect on infected tadpoles (25, 26), but Bd can lead to the death of postmetamorphic animals of many species within weeks of infection (2, 6, 27).

Here we investigate how infected *R. sierrae* populations are able to persist with Bd. We present a 5-year field study that reveals that adults in persistent populations are infected with only low-level infections (low Bd load), and individuals frequently lose and regain the infection. This is in stark contrast to

Author contributions: C.J.B., R.A.K., and V.T.V. designed research; C.J.B. performed research; C.J.B. analyzed data; and C.J.B. wrote the paper.

The authors declare no conflict of interest.

*This Direct Submission article had a prearranged editor.

Freely available online through the PNAS open access option.

[1]To whom correspondence should be addressed. E-mail: briggs@lifesci.ucsb.edu.

This article contains supporting information online at www.pnas.org/lookup/suppl/doi:10.1073/pnas.0912886107/-/DCSupplemental.

the dynamics observed during frog die-offs, during which individuals rapidly build up high-level infections, followed by death due to chytridiomycosis (16). These observations motivated the development of a model that incorporates the Bd load dynamics on individual frogs. Previous models of Bd–frog interactions (17, 28) have followed the standard assumption of most microparasite models that host individuals can be categorized simply as susceptible, infected, or recovered, ignoring the dynamics of the pathogen within a host individual. For Bd, infection intensity strongly determines the infectivity of individuals and outcome of infection (27, 29). In most microparasite models, once an individual is infected, reexposure of the infected host to the pathogen does not affect disease progression. But Bd appears to lack an efficient mechanism to transmit between cells within an infected host (21, 30); increasing intensity of infection depends mainly on reinfection from zoospores released within the skin and onto the skin surface or infection from aquatic zoospores. Thus, the Bd–frog interaction includes aspects typical of both macroparasites and microparasites. Our model includes details of the dynamics of zoospore density in the environment and fungal load dynamics within individuals. This model can easily incorporate the effects of temperature (23, 31) or other environmental conditions (such as water flow rate) on Bd growth. We use the model to investigate the conditions that allow for population persistence versus extirpation after the invasion of Bd.

Results

Mark-Recapture Study: Survival and Persistence with Bd. In a 5-year study, a total of 392 adult *R. sierrae* were tagged at three persistent Bd-infected sites. Each site had consistently small *R. sierrae* population counts; the average number of adult frogs observed per visit was only 8 (± 1 SE) at site 1, 23 (± 4) at site 2, and 31 (± 5) at site 3. But reproduction occurred each year, and tadpoles were present every year. On average, 60% of the adult frogs at site 1, 76% of those at site 2, and 74% of those at site 3 were infected on each sample date (Fig. 1 *A–C*). No consistent seasonal trend in the prevalence of adult infection was observed; the prevalence increased significantly from the start to the end of the summer season only at site 3 [logistic regression: logit(prevalence at site 3) = 0.18 + 0.01 · days since June 1 of the year; $P < 0.01$].

Infected adult frogs frequently lost and gained Bd infection through time (Fig. 1*E*). Of the 215 frogs that were captured more than once, 95.0% were infected during at least one of the capture events, but 38.6% transitioned from being infected to being uninfected at least once during the study, and 41.9% made the transition from uninfected to infected. Infected adults had low infection intensities as measured by the number of zoospore equivalents detected by real-time PCR on a standardized skin swab, termed "Bd load" (Fig. 1 *A–E*). The mean Bd load on infected adults across the three sites was 220 (± 81) zoospore equivalents per standardized swab, with a median value of only 20.5 zoospore equivalents (including all individuals with a snout-to-vent length ≥ 40 mm). These levels are much lower than the Bd loads reported in a recent study of *R. muscosa*/*R. sierrae* populations elsewhere in the Sierra Nevada during massive die-offs (16). In that study, after the first appearance of Bd, zoospore load increased approximately exponentially until the average zoospore load reached 10^4 to 10^5 per standardized swab, at which point the frog populations collapsed, in many cases to extirpation. In the current study, only two adult frogs at any of the persistent sites were ever observed to have a Bd load exceeding 10^4 per standardized swab. In contrast, the tadpoles and recently metamorphed individuals had significantly higher Bd loads compared with adults [Fig. 1*D*; ANOVA on log-transformed Bd loads on individuals with a Bd load >0, $P < 0.01$; tadpoles: mean, 4,013 ± 289, median, 1,744 zoospores per standardized swab; metamorphs (individuals with Gosner stage 45 or 46 with a snout-to-

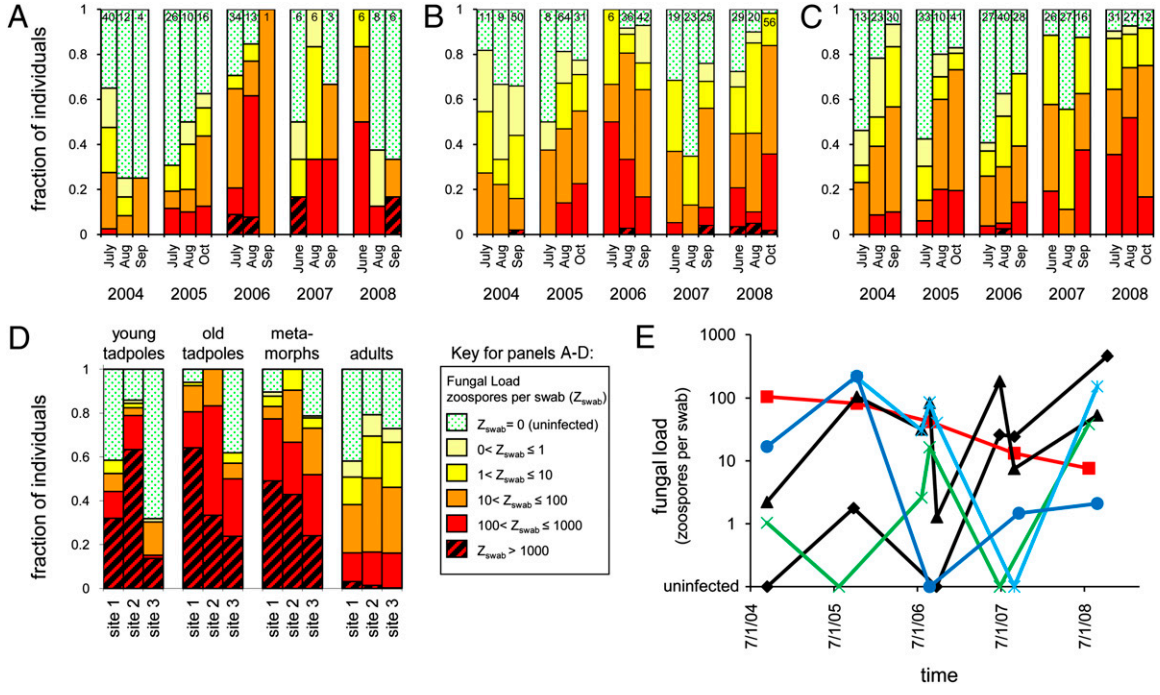

Fig. 1. Bd load data from *R. sierrae* at sites with enzootic infections. (*A–C*) Infection prevalence and distribution of Bd loads in adult *R. sierrae* at three sites over 5 years. The number of individuals swabbed is shown at the top of each bar. The distribution of Bd load, as measured by the numbers of zoospores per swab (Z_{swab}) as estimated by real-time PCR is shown in the colored bars. (*D*) Comparison of the fungal load in young tadpoles (Gosner stage ≤ 37), old tadpoles (Gosner stage 38–41), metamorphs, and adults at the three sites for all dates combined. Bd loads on subadults (postmetamorphic individuals with a snout-to-vent length of 35–40 mm) was not significantly different from those on adult frogs, and subadults and adults are combined in the figure. (*E*) Examples of changes in Bd load through time for individually marked adult *R. sierrae*. Shown are Bd loads for six of the individuals at site 3 that were captured in multiple years.

vent length <35 mm): mean, 4,913 ± 820; median, 631 zoospores per standardized swab).

The most important result from the multistate mark-recapture analysis (32) was that Bd infection status had no detectable effect on adult frog survival at these persistent sites (likelihood ratio test comparing a model in which the survival probability depends on infection status and site with one in which the survival probability depends only on site; $\chi^2 = 1.5$, df = 3, $P > 0.6$). The survival rates were significantly different between the sites, however (likelihood ratio test comparing models in which survival probability varied between sites with model with a constant survival rate; $\chi^2 = 15.9$, df = 2, $P < 0.001$), with best estimates of annual adult survival probabilities of 48.2% at site 1, 79.4% at site 2, and 86.5% at site 3. The "best model" from the mark-recapture analysis was one in which the adult frog survival probability depended only on site and not on infection status or time, the state transition probabilities depended on infection status (with the monthly transition rate from uninfected to infected higher at each site than the monthly transition rate from infected to uninfected) and site, and the capture probabilities depended on site and time (due to variability in survey conditions and capture effort). The model comparisons, best estimates, and 95% confidence intervals (CIs) for all model parameters are provided in *SI Methods*.

Bd Load Model. The Bd load model follows the number of zoospores in a zoospore pool (i.e., a lake or pond containing a population of frogs), and the number of sporangia on each frog (Fig. 2*A*). The model describing the zoospore dynamics in a single frog in a zoospore pool is a set of linear ordinary differential equations, and thus the only two potential outcomes are exponential growth (resulting in death of the frog when the number of sporangia reaches the maximum level that a frog can tolerate, S_{max}) or exponential decline (loss of infection) at rate λ (the dominant eigenvalue of the linear system). Exponential growth of sporangia on a single frog ($\lambda > 0$) occurs if the zoospore release and reinfection rates are greater than the loss rates of sporangia from the frog skin. Local environmental conditions, including temperature, humidity, and/or water flow rate are likely to affect the reinfection and loss rates, such that individuals of a given species of amphibian may die due to the infection in some environmental conditions, but lose the infection in other conditions (Fig. 2*B*).

The growth rate of Bd (λ) is an increasing function of frog density (Fig. 2*C*). For encounter and reinfection rates for which Bd on a single frog has a negative growth rate, there is a threshold frog population size, N_T, above which the Bd growth rate shifts from negative to positive. Increasing the number of frogs further above N_T also decreases the time needed for the density of sporangia on each frog to reach S_{max} (i.e., the time to death due to chytridiomycosis decreases). Thus, the inclusion of Bd load dynamics in this model can explain the rapid mortality due to Bd in some frog populations (especially when Bd first invades large, uninfected populations), but survival and potential recovery of frogs in others. The death of frogs when their Bd load exceeds S_{max} creates a negative feedback, such that it is possible for disease-induced mortality to reduce the frog population size to below N_T; however, persistence of the pathogen would then require a delicate balance between mortality due to chytridiomycosis and replenishment of the host population through reproduction. Investigating this requires additional assumptions about frog reproduction and mortality; a number of variants were evaluated.

Unstructured host model. In the simplest version, there is no stage structure in the host population, and frog reproduction occurs in a discrete pulse each year. With an unstructured host population, persistence of an infected frog population for even a decade is possible for only a narrow range of parameters (Fig. 3*A*) with relatively low self-reinfection rates and intermediate zoospore encounter rates. With very low encounter rates, Bd goes extinct, and for higher encounter rates, Bd rapidly drives the frogs toward extinction. For parameters in the persistent region, within a year the fungal load on a fraction of the individuals grows exponentially (e.g., black line in Fig. 3*B*) until $S_{\max}$ is reached, at which point those frogs die, whereas the fungal loads on another fraction of the individuals (e.g., red, blue, and green lines in Fig. 3*B*) fluctuate at low levels, and in many cases individuals temporarily become uninfected and are subsequently reinfected.

Model with an external source of zoospores. Long-term persistence is a more likely outcome if there is some mechanism present to keep the pathogen from going extinct during the troughs of zoospore density. An external source of zoospores, from either an environmental reservoir for Bd (an environmental reservoir for Bd has not yet been found, although this remains a possibility) or a more resistant alternative amphibian host that contributes a constant input of zoospores into the zoospore pool, can result in persistence of an infected frog population over a wide range of parameter values (Fig. 3*C*). For low values of the zoospore encounter rate, individual frogs can repeatedly gain and lose the infection without ever reaching the high fungal loads at which Bd causes mortality (Fig. 3*D*). This pattern is consistent with what we observe in persistent mountain yellow-legged frog populations.

Model with a long-lived tadpole stage. A long-lived tadpole stage that can become infected but not succumb to infection also can

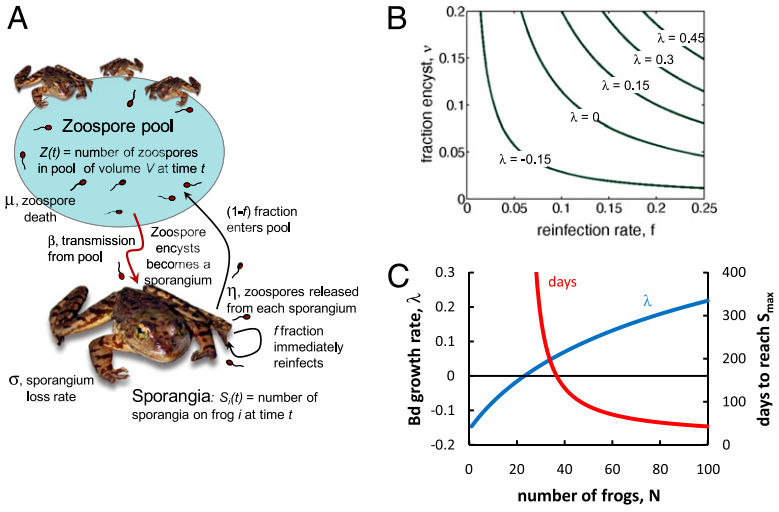

Fig. 2. The Bd load model, and results from the deterministic version within a year. (*A*) Diagram of the within-host/zoospore pool model. (*B*) Growth rate of Bd on individual frogs (λ), as a function of *f*, the fraction of zoospores that reencounter the host from which they were released, and ν, the fraction of zoospores that successfully infect the frog skin on encountering a host. Other parameters are $V = 1$ unit volume, $\gamma = 0.01$ unit volume · day^{-1}, $\mu = 1$ day^{-1}, $\eta = 17.5$ zoospores · day^{-1}, and $\sigma = 0.2$ day^{-1}. (*C*) Growth rate, λ, of Bd in the zoospore pool and time to reach $S_{\max} = 10{,}000$ sporangia as a function of frog density. Parameters are as in *B*, with $\nu = 0.05$ and $f = 0.05$. With few frogs present, the growth of Bd on each frog is negative, and all frogs will clear the infection. Above a density of ~20 frogs, the Bd growth rate is positive on each frog. Also shown is the number of days that it takes for the density of sporangia on each frog to reach $S_{\max}$.

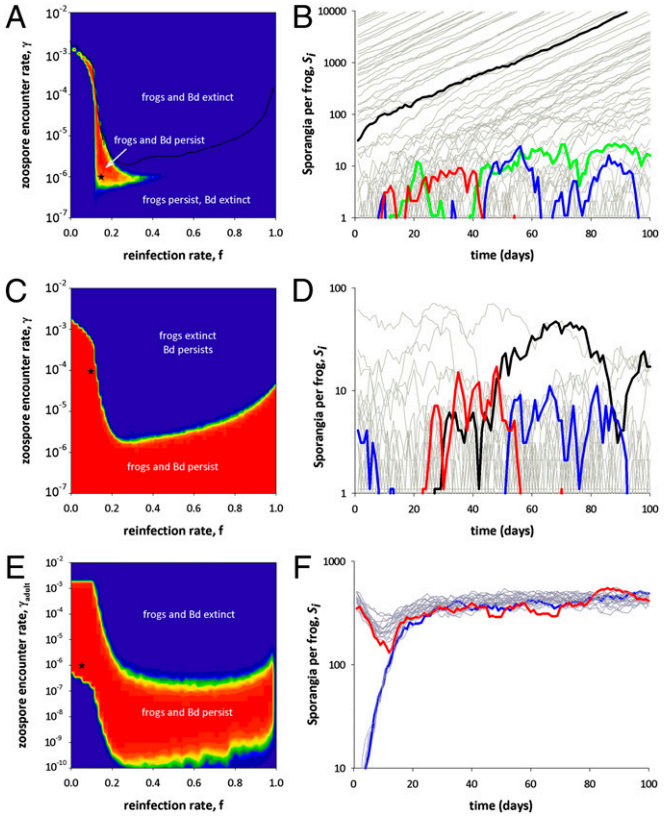

Fig. 3. Probability of persistence, and sample within-season trajectories for three different variants of the stochastic model. (*A*, *C*, and *E*) Probability of frogs and Bd persisting for at least 10 years as a function of reinfection rate, *f*, and zoospore encounter rate, γ. Shown are the fractions of 100 runs for each combination of parameters that persist for at least 10 years (red, 100% of runs persist; blue, 0% of runs persist). All runs are initialized with a single infected frog in an otherwise uninfected frog population at its carrying capacity and no zoospores in the zoospore pool ($Z = 0$). In all of the models, the frog population can be rapidly driven extinct at high values of the zoospore encounter rate (high γ). (*B*, *D*, and *F*) Examples of within-season dynamics showing the dynamics of the number of sporangia on individual frogs. The colored lines are highlighted examples of trajectories of sporangia on individual frogs. (*A* and *B*) Unstructured host model, with $R = 4$, $K = 100$ frogs, $\theta_F = 0.9$, $\theta_Z = 0.1$, $V = 1$ unit volume, $\nu = 0.1$, $\mu = 1$ day^{-1}, $\eta = 17.5$ zoospores · day^{-1}, and $\sigma = 0.2$ day^{-1}. In *B*, $f = 0.15$, $\gamma = 1 \times 10^{-6}$ unit volume · day^{-1}. (*C* and *D*) Model with external source of zoospores. All parameters are as in *A*, with $\varepsilon_Z = 1{,}000$ zoospores. In *D*, $f = 0.1$, $\gamma = 1 \times 10^{-4}$ unit volume · day^{-1}. (*E* and *F*) Model with long-lived tadpole stage. In *F*, $f = 0.05$ for both tadpoles and adults, $\gamma_{adult} = 1 \times 10^{-6}$ unit volume · day^{-1}, $\gamma_{tadpole} = 100 \cdot \gamma_{adult}$, $\nu_{adult} = \nu_{tadpole} = 0.1$, $S_{max\_adult} = S_{max\_tadpole} = 10{,}000$ sporangia, $R = 40$ tadpoles, $\theta_{adult} = 0.9$, $\theta_{tadpole} = 0.2$, $\theta_Z = 0.1$, $m = 0.5$, $V = 1$ unit volume, $\gamma = 0.01$ unit volume · day^{-1}, $\mu = 1$ day^{-1}, $\eta = 17.5$ zoospores · day^{-1}, and $\sigma = 0.2$ day^{-1}. Stars in *A*, *C*, and *E* indicate parameter values used for simulations in *B*, *D*, and *F*, respectively.

promote pathogen persistence (Fig. 3*E*). In this model variant, we assume that both tadpoles and adults become infected by, and contribute to, the zoospore pool, but that tadpoles do not die when their Bd load reaches the maximum number of zoospores per tadpole. As such, tadpoles can act as a within-host reservoir for the pathogen, producing zoospores that can infect susceptible adults. Model results show that the pathogen can persist on a stage-structured host population across a wide range of parameters, especially when transmission rates are relatively low (Fig. 3*E*). In the persistent region of parameter space with low self-reinfection rates, the tadpoles continually transmit zoospores to the adult population, maintaining low to intermediate zoospore loads on adults (e.g., the red line in Fig. 3*F*), with no adult mortality due to Bd. Newly recruited adults rapidly become infected with low zoospore loads (e.g., the blue line in Fig. 3*F*).

Model with full R. Muscosa/R. Sierrae stage structure. In a variant of the model with the full frog stage structure (17), the potential for persistence is again enhanced by the multiyear tadpole stage. Figure 4 shows three examples of the types of model dynamics observed in field populations of *R. muscosa*/*R. sierra*, where the only difference leading to the different trajectories is a change in the transmission parameter, γ. In Fig. 4*A*, subadults survive to recruit to the reproductive adult stage only occasionally, whereas Bd loads on adults never reach the lethal level. In the model, this occurs when zoospores encounter and successfully infect subadults at a higher rate, but subadults die of chytridiomycosis at a lower fungal load (i.e., lower S_{max}) than adults. In Fig. 4*B*, frogs and Bd remain extant for many years after arrival of Bd at a site, but subadults never recruit to the adult stage, and the apparently persistent population is actually on a slow decline to extinction. Figure 4*C* shows an example of the type of dynamics observed in many *R. muscosa*/*R. sierrae* populations that rapidly go extinct after the arrival of Bd. Adults and subadults reach high Bd loads and die shortly after Bd arrival. All individuals in each tadpole class die due to chytridiomycosis as soon as they reach metamorphosis, and the population is completely extinct within 2–3 years. This occurs when the adults encounter zoospores at a high rate.

Discussion

Our model offers insight into the epidemic and endemic dynamics of Bd, a widespread and sometimes devastating pathogen. At many sites, the first arrival of Bd into an uninfected frog population coincides with an outbreak of chytridiomycosis, during which the Bd loads in susceptible individuals increase rapidly (16). The model predicts that this buildup of infection intensity will occur more rapidly in dense frog populations and under

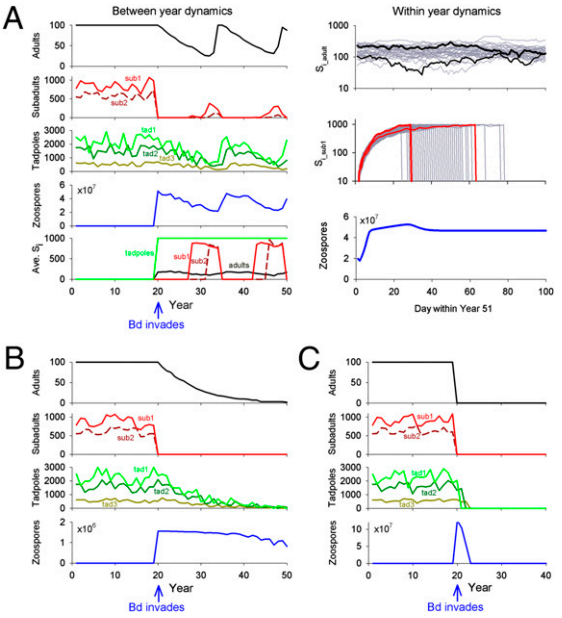

Fig. 4. Examples of dynamics of model with full-stage *R. muscosa*/*R. sierra* structure. The simulation starts with the population uninfected, and Bd invades during year 20 of the simulation. For *A*, the within-season dynamics are also shown for a single year (year 51). Thick lines in the within-season dynamics plots are simply trajectories of highlighted individuals for illustrative purposes. In *A*, $\gamma_{adult} = 1 \times 10^{-6}$ unit volume · day^{-1}, $\gamma_{subadult} = 10 \cdot \gamma_{adult}$, $\gamma_{tadpole} = 100 \cdot \gamma_{adult}$, $S_{max\_adult} = 10{,}000$, $S_{max\_subadult} = S_{max\_tadpole} = 1{,}000$. In B. $\gamma_{adult} = 1 \times 10^{-4}$ unit volume · day^{-1}, $\gamma_{subadult} = 10 \cdot \gamma_{adult}$, $\gamma_{tadpole} = 100 \cdot \gamma_{adult}$, $S_{max\_adult} = 10{,}000$, and $S_{max\_subadult} = S_{max\_tadpole} = 1{,}000$. In *C*, $\gamma_{adult} = \gamma_{subadult} = \gamma_{tadpole} = 1 \times 10^{-3}$ unit volume · day^{-1}, $S_{max\_adult} = S_{max\_subadult} = S_{max\_tadpole} = 10{,}000$, $\theta_{adult} = 0.9$, $\theta_{sub1} = \theta_{sub2} = 0.7$, $\theta_{tad1} = \theta_{tad2} = \theta_{tad3} = 0.7$, $\theta_Z = 0.5$, $m = 0.5$, $\omega_{metamorph} = 0.9$, $p_F = 0.25$, $R = 100$, $K = 100$, $f = 0.1$, $\nu = 0.1$, $\eta = 17.5$ zoospores · day^{-1}, $\sigma = 0.2$ day^{-1} for all frog stages, $V = 1$ unit volume, and $\mu = 1$ day^{-1}.

conditions that promote the continual reinfection of infected individuals (e.g., small volumes of nonflowing water). If the Bd load on all individuals reaches a high level, then extinction of the frog population can occur; however, if some individuals survive the initial epidemic, then persistence of the infected amphibian population in a new endemic state is possible.

Similar endemic Bd dynamics after drastic population declines have been reported in the Eungella torrent frog (*Taudactylus eungellensis*) in Australia (33); that study suggested that evolution of resistance in the frogs or evolution of less-pathogenic strains of Bd might have been responsible. But our model suggests that the different population-level outcomes of Bd infection within the same species do not require differences in frog susceptibility, pathogen virulence, or environmental conditions (although each of these might play a role), and might simply represent epidemic and endemic dynamics of the same host–pathogen interaction. A recent mark-recapture study on another Australian frog species, *Litoria pearsoniana*, over a single season, found that Bd reduced the monthly survival of infected individuals in an endemically infected population by 38% (34). Our model suggests that understanding the within-host fungal load dynamics is the key to understanding the different impacts of Bd between systems and to determining the mechanisms of persistence versus extinction.

In the Sierra Nevada, we are currently seeing both epidemic and endemic Bd dynamics. In some regions (e.g., much of Sequoia and Kings Canyon National Park; ref. 16), Bd is apparently invading for the first time, and the most common outcome of Bd epidemics is extirpation of *R. muscosa*/*R. sierrae* populations. But not all newly infected populations have gone extinct, and there remains hope that some of these populations might persist with Bd in an endemic state. In other areas, Bd arrived at some time in the past, and the initial epidemic phase of its dynamics was not observed. In Yosemite National Park, *R. sierrae* has persisted in only a fraction of its suitable habitat, and the remaining populations are all infected with Bd. Some of these populations might be on a slow drift to extinction, but others may be truly persisting with Bd in an endemic state. Several of the results of the model with the full *R. muscosa*/*R. sierrae* stage structure are consistent with our field observations. At persistent sites, infected adults have low Bd loads, only very rarely reaching the lethal level. Tadpoles and subadults have high Bd loads, however, and Rachowicz et al. (6) showed experimentally that *R. muscosa*/*R. sierrae* suffer high rates of mortality during metamorphosis in both persistent and nonpersistent populations. The model suggests that the pattern of repeated loss and regain of infection observed in adults at field sites might be explained by repeated reinfection of adults from long-lived infected tadpoles. Given the lack of a detectable effect of Bd on adult frog survival in persistent populations, the main impact of Bd on *R. muscosa*/*R. sierrae* in populations persisting with Bd appears to occur during metamorphosis, and this increased mortality at metamorphosis might be responsible for the generally small population sizes at these sites.

Our model highlights the crucial parameters to measure to gain insight into Bd dynamics (including the rate of buildup of Bd load on individuals and the rate of shedding of zoospores into the zoospore pool). The model also can be modified to help interpret a number of experimental or observational studies investigating how such factors as temperature (23, 35), moisture, water flow rate, frog behavior (14, 36), and zoospore dose (27) can influence the growth rate of Bd and thus the outcome of infection. Model development also suggests mechanisms that we have omitted but that might alter the dynamics and should be explored further (e.g., an adaptive immune response, or any process that regulates the fungal load on individuals to something other than exponential growth/decline). The model presented here does not include adaptive immunity by the frogs against Bd, in part because we sought to determine whether frog population persistence despite Bd could be explained without invoking an immune response. In addition, empirical evidence for an adaptive immune response is still lacking. Recent studies involving gene expression profiling of uninfected frogs and those infected with Bd have found no evidence of up-regulation of genes associated with an adaptive immune response (37, 38), although these studies were limited to one highly succeptible frog species (*Silurana tropicalis*). This potential explanation for endemic persistence will merit further investigation if future studies demonstrate the presence of adaptive immunity against Bd.

This study also provides a useful new modeling framework for investigating conservation strategies to protect amphibian populations worldwide. Although it appears that Bd has already arrived in many areas of the world, there remain some regions where it has not yet been detected (39, 40). Therefore, strategies that reduce the Bd load if and when it arrives (e.g., treating individuals with antifungal compounds, reducing population density, or temporarily removing tadpoles) might permit some individuals to survive the initial epidemic and allow the population to persist with an endemic Bd infection.

Methods

Mark-Recapture Study. We performed a mark-recapture study on *R. sierrae* for five summers (2004–2008) at three "persistent" sites in the Sierra Nevada of California that have had Bd-infected frog populations for several years: site 1, Little Indian Valley, 38°35′45″N, 119°53′15″W, elevation 2,425 m; site 2, Mono Pass, Yosemite National Park, 37°51′15″N, 119°13′14″W, elevation 3,235 m; and site 3, Unicorn Basin, Yosemite National Park, 37°50′36″N, 119°23′06″W, elevation 3,070 m. Each site was visited at least three times per summer during the ice-free months (June–October, depending on year). Counts of all lifestages of *R. sierrae* and other amphibians observed on each visit were recorded. *R. sierrae* was by far the numerically dominant amphibian at these sites, although *Pseudacris regilla* (sites 1 and 2), *Bufo canorus* (sites 2 and 3), and *Ambystoma macrodactylum* (site 1) were observed in small numbers. On each visit, as many adult *R. sierra* as possible were individually captured with hand-held nets. All frogs with snout-to-vent length >48 mm were individually marked with passive integrated transponder (PIT) tags (cylinders 12 mm long × 2 mm in circumference; AVID), which contain unique nine-digit numbers that are detected and read with hand-held readers. A total of 392 adult *R. sierrae* were tagged (*SI Methods*). On first capture, a PIT tag was inserted beneath the skin through a small incision on the dorsal surface just posterior to the head and moved subcutaneously to behind the dorsal pelvic girdle. The weight, snout-to-vent length, sex, and any obvious symptoms of disease (e.g., lack of righting reflex) were recorded for each frog.

To determine infection status, each frog was swabbed with a synthetic swab (Medical Wire & Equipment) using a standardized swabbing protocol involving a total of 30 strokes (5 strokes on each of the hind foot, thigh of the hind leg, and side of the abdomen on the ventral side). After swabbing, each frog was returned to its place of capture. Each swab was allowed to air dry and then was placed in an individually labeled vial and put on ice or in a freezer as soon as possible (41). The number of copies of Bd DNA on each swab (i.e., the Bd load) was determined using real-time quantitative PCR following the protocol of Boyle et al. (42), and the Bd load was adjusted to account for the fraction of the extract from the swab used in the PCR. A threshold of 0 zoospore equivalents of Bd DNA on the swab served as the cutoff, above which a frog was designated as Bd-positive on that sampling date. The PCR assay consistently detected very small Bd loads (0–1) on a fraction of swabs. Measurements of these low fungal loads are repeatable and likely represent very low levels of infection.

A multistate model, based on the Cormack–Jolly–Seber method (32), was implemented using the MARK program (http://welcome.warnercnr.colostate.edu/~gwhite/mark/mark.htm) to investigate the effect of Bd infection status on adult frog survival. For this analysis, the encounter history of each frog was compiled for each of three time periods (early, mid, and late summer) over the 5 years (15 capture events per frog). If more than three surveys were performed at a site in a given year, then the surveys were pooled into early, mid, and late summer periods. During each of the 15 capture events, each frog was classified as Bd-infected (I), Bd-uninfected (U), or not captured (0). The model contained three types of parameters: survival probabilities, transition probabilities, and recapture probabilities (*SI Methods*). A maximum likelihood approach was used to determine the values of the parameters for a given model that best explained the observed encounter histories, and model selection using the corrected Akaike information criterion (AICc) was used to compare models in which each of the model parameters was constant or allowed to vary with site, infection status, and/or time.

Bd Load Model. Our model (Fig. 2*A*) follows the number of zoospores, Z, in a zoospore pool (i.e., a lake or pond containing a population of frogs), and the number of sporangia, S_i, on each frog i. Zoospores from the pool encounter frogs at rate γ, and a fraction, ν, of those zoospores successfully infect the frog skin and become sporangia, such that the rate of successful transmission is $\beta = \nu\,\gamma$. The remaining fraction of zoospores that encounter frogs $(1 - \nu)$ might be killed by the frogs' defenses, such as antimicrobial peptides (11) or bacteria on the frogs' skin (12). Each sporangium releases zoospores at rate η. A fraction, f, of the released zoospores immediately encounters the same host (and a fraction, ν, of these zoospores successfully infects the frog skin), whereas the remaining fraction, $(1 - f)$, enters the zoospore pool. Sporangia are lost from infected hosts at rate σ, which incorporates the mortality rate of sporangia and the rate at which infected hosts shed skin. Zoospores also are lost from the pool through mortality or attachment to inappropriate substrates at rate μ, such that the average lifespan of a zoospore in the environment is $1/\mu$. Chytridiomycosis is a disease of only the frog skin that appears to lead to mortality through interference with electrolyte transport across the epidermis (29). Our default assumption is that an individual frog can tolerate only $S_{\max}$ zoospores on its skin before it succumbs to chytridiomycosis and dies (consistent with refs. 27 and 29).

The equations for the deterministic version of the model (Fig. 2*A*) describing the dynamics in a zoospore pool of volume V are $dS_i/dt = (\beta/V)\,Z + \eta\,\nu\,f\,S_i - \sigma\,S_i$ for $i = 1 \ldots N$, $S_i \leq S_{\max}$, and $dZ/dt = \sum_{i=1}^{N}[\eta(1-f)S_i] - (\gamma/V)\,NZ - \mu Z$, where N is the number of frogs currently present in the population. To allow for stochasticity, in the model simulations time is discretized into short time steps, Δt. Details of the model simulations and sources of parameter estimates are given in *SI Methods*.

The following variants of the model were investigated. Details are provided in *SI Methods*.

Unstructured host model. In the simplest version, there is no stage structure in the host population, and frog reproduction occurs in a discrete pulse each year.

Model with an external source of zoospores. An external source of zoospores was incorporated into the unstructured host model through the addition of a number of zoospores drawn from a Poisson distribution with mean ε_Z to the zoospore pool each day. This addition can represent either an environmental reservoir for the pathogen or transmission of zoospores from an alternative amphibian host with an approximately constant density that is unaffected by the pathogen.

Model with a long-lived tadpole stage. In this variant, the frog population is structured into a tadpole stage and an adult stage, both of which contribute zoospores to the same zoospore pool; however, tadpoles do not die when their Bd load reaches the maximum number of zoospores per tadpole.

Model with full R. Muscosa/R. Sierrae age structure. In this variant of the model, we incorporate the full-stage structure of the *R. muscosa*/*R. sierrae* system, as in Briggs et al. (17).

ACKNOWLEDGMENTS. We thank John Latto, Tate Tunstall, Mary Stice, Mary Toothman, Tom Smith, Lara Rachowicz, Natalie Reeder, and the National Park Service (especially the Yosemite National Park staff) for their assistance with varied aspects of this research. This work was funded by National Institutes of Health (NIH)/National Science Foundation (NSF) Ecology of Infectious Disease Program Grants R01 ES012067 from the NIH National Institute of Environmental Health Sciences and EF-0723563 from the NSF.

1. Gascon C, et al., eds. (2007) *Amphibian Conservation Action Plan.* Proceedings of the IUCN.SSC Amphibian Conservation Summit 2005 (World Conservation Union, Gland, Switzerland). Available at http://intranet.iucn.org/webfiles/doc/SSC/SSCwebsite/GAA/ACAP_Summit_Declaration.pdf. Accessed November 1, 2009.
2. Berger L, et al. (1998) Chytridiomycosis causes amphibian mortality associated with population declines in the rain forests of Australia and Central America. *Proc Natl Acad Sci USA* 95:9031–9036.
3. Longcore JE, Pessier AP, Nichols DK (1999) *Batrachochytrium dendrobatidis* gen. et sp. nov., a chytrid pathogenic to amphibians. *Mycologia* 91:219–227.
4. Rachowicz LJ, et al. (2005) The novel and endemic pathogen hypotheses: Competing explanations for the origin of emerging infectious diseases of wildlife. *Conserv Biol* 19:1441–1448.
5. Skerratt LF, et al. (2007) Spread of chytridiomycosis has caused the rapid global decline and extinction of frogs. *EcoHealth* 4:125–134.
6. Rachowicz LJ, et al. (2006) Emerging infectious disease as a proximate cause of amphibian mass mortality. *Ecology* 87:1671–1683.
7. Lips KR, et al. (2006) Emerging infectious disease and the loss of biodiversity in a neotropical amphibian community. *Proc Natl Acad Sci USA* 103:3165–3170.
8. Daszak P, et al. (2004) Experimental evidence that the bullfrog (*Rana catesbeiana*) is a potential carrier of chytridiomycosis, an emerging fungal disease of amphibians. *Herpetol J* 14:201–207.
9. Weldon C, du Preez LH, Hyatt AD, Muller R, Speare R (2004) Origin of the amphibian chytrid fungus. *Emerg Infect Dis* 10:2100–2105.
10. Berger L, et al. (2004) Effect of season and temperature on mortality in amphibians due to chytridiomycosis. *Aust Vet J* 82:434–439.
11. Woodhams DC, et al. (2007) Resistance to chytridiomycosis varies among amphibian species and is correlated with skin peptide defenses. *Anim Conserv* 10:409–417.
12. Harris RN, James TY, Lauer A, Simon MA, Patel A (2006) Amphibian pathogen *Batrachochytrium dendrobatidis* is inhibited by the cutaneous bacteria of amphibian species. *EcoHealth* 3:53–56.
13. Kriger KM, Hero J-M (2007) The chytrid fungus *Batrachochytrium dendrobatidis* is non-randomly distributed across amphibian breeding habitats. *Divers Distrib* 13:781–788.
14. Rowley JJL, Alford RA (2007) Behaviour of Australian rainforest stream frogs may affect the transmission of chytridiomycosis. *Dis Aquat Organ* 77:1–9.
15. Lips KR, Reeve JD, Witters LR (2003) Ecological traits predicting amphibian population declines in Central America. *Conserv Biol* 17:1078–1088.
16. Vredenburg VT, Knapp RA, Tunstall TS, Briggs CJ (2010) Dynamics of an emerging disease drive large-scale amphibian population extinctions. *Proc Natl Acad Sci USA*, 10.1073/pnas.0914111107.
17. Briggs CJ, Vredenburg VT, Knapp RA, Rachowicz LJ (2005) Investigating the population-level effects of chytridiomycosis: An emerging infectious disease of amphibians. *Ecology* 86:3149–3159.
18. Fellers GM, Green DE, Longcore JE (2001) Oral chytridiomycosis in the mountain yellow-legged frog (*Rana muscosa*). *Copeia* 2001:945–953.
19. Ouellet M, Mikaelian I, Pauli BD, Rodrigue J, Green DM (2005) Historical evidence of widespread chytrid infection in North American amphibian populations. *Conserv Biol* 19:1431–1440.
20. Vredenburg VT, et al. (2007) Concordant molecular and phenotypic data delineate new taxonomy and conservation priorities for the endangered mountain yellow-legged frog. *J Zool (Lond)* 271:361–374.
21. Berger L, Hyatt AD, Speare R, Longcore JE (2005) Life cycle stages of the amphibian chytrid *Batrachochytrium dendrobatidis*. *Dis Aquat Organ* 68:51–63.
22. Piotrowski JS, Annis SL, Longcore JE (2001) Physiology, zoospore behavior, and enzyme production of *Batrachochytrium dendrobatidis*, a chytrid pathogenic to amphibians. *Phytopathology* 91:S121.
23. Woodhams DC, Alford RA, Briggs CJ, Johnson M, Rollins-Smith LA (2008) Life-history trade-offs influence disease in changing climates: Strategies of an amphibian pathogen. *Ecology* 89:1627–1639.
24. Di Rosa I, Simoncelli F, Fagotti A, Pascolini R (2007) Ecology: The proximate cause of frog declines? *Nature* 447:E4–E5.
25. Rachowicz LJ, Vredenburg VT (2004) Transmission of *Batrachochytrium dendrobatidis* within and between amphibian life stages. *Dis Aquat Organ* 61:75–83.
26. Blaustein AR, et al. (2005) Interspecific variation in susceptibility of frog tadpoles to the pathogenic fungus *Batrachochytrium dendrobatidis*. *Conserv Biol* 19:1460–1468.
27. Carey C, et al. (2006) Experimental exposures of boreal toads (*Bufo boreas*) to a pathogenic chytrid fungus (*Batrachochytrium dendrobatidis*). *EcoHealth* 3:5–21.
28. Mitchell KM, Churcher TS, Garner TWJ, Fisher MC (2008) Persistence of the emerging pathogen *Batrachochytrium dendrobatidis* outside the amphibian host greatly increases the probability of host extinction. *Proc R Soc Biol Sci B* 275:329–334.
29. Voyles J, et al. (2009) Pathogenesis of chytridiomycosis, a cause of catastrophic amphibian declines. *Science* 326:582–585.
30. Berger L, Speare R, Skerratt LF (2005) Distribution of *Batrachochytrium dendrobatidis* and pathology in the skin of green tree frogs *Litoria caerulea* with severe chytridiomycosis. *Dis Aquat Organ* 68:65–70.
31. Pounds JA, et al. (2006) Widespread amphibian extinctions from epidemic disease driven by global warming. *Nature* 439:161–167.
32. Nichols J, Hines JE, Pollock KH, Hinz RL, Link WA (1994) Estimating breeding proportions and testing hypotheses about costs of reproduction with capture-recapture data. *Ecology* 75:2052–2065.
33. Retallick RWR, McCallum H, Speare R (2004) Endemic infection of the amphibian chytrid fungus in a frog community post-decline. *PLoS Biol* 2:1965–1971.
34. Murray KA, Skerratt LF, Speare R, McCallum H (2009) Impact and dynamics of disease in species threatened by the amphibian chytrid fungus, *Batrachochytrium dendrobatidis*. *Conserv Biol* 32:1242–1252.
35. Piotrowski JS, Annis SL, Longcore JE (2004) Physiology of *Batrachochytrium dendrobatidis*, a chytrid pathogen of amphibians. *Mycologia* 96:9–15.
36. Richards-Zawacki CL (2010) Thermoregulatory behaviour affects prevalence of chytrid fungal infection in a wild population of Panamanian golden frogs. *Proc R Soc Biol Sci B* 277:519–528.
37. Rosenblum EB, et al. (2009) Genome-wide transcriptional response of *Silurana* (*Xenopus*) *tropicalis* to infection with the deadly chytrid fungus. *PLoS One* 4:e6494.
38. Ribas L, et al. (2009) Expression profiling the temperature-dependent amphibian response to infection by *Batrachochytrium dendrobatidis*. *PLoS One* 4:e8408.
39. Weldon C, Du Preez LH, Vences M (2008) Lack of detection of the amphibian chytrid fungus (*Batrachochytrium dendrobatidis*) in Madagascar. *A Conservation Strategy for the Amphibians of Madagascar*, ed Andreone F (Museo Regionale di Scienze Naturali, Turin, Italy), pp 95–106.
40. Rowley JJL, et al. (2007) Survey for the amphibian chytrid *Batrachochytrium dendrobatidis* in Hong Kong in native amphibians and in the international amphibian trade. *Dis Aquat Organ* 78:87–95.
41. Hyatt AD, et al. (2007) Diagnostic assays and sampling protocols for the detection of *Batrachochytrium dendrobatidis*. *Dis Aquat Organ* 73:175–192.
42. Boyle DG, Boyle DB, Olsen V, Morgan JAT, Hyatt AD (2004) Rapid quantitative detection of chytridiomycosis (*Batrachochytrium dendrobatidis*) in amphibian samples using real-time Taqman PCR assay. *Dis Aquat Organ* 60:141–148.